Forensic Science International 293 (2018) 27–36

Contents lists available at ScienceDirect

Forensic Science International

journal homepage: www.elsevier.com/locate/forsciint

Determination of the maximum distance blood spatter travels from a vertical impact

Chris Flight[a,*], Max Jones[b], Kaye N. Ballantyne[a]

[a] Office of the Chief Forensic Scientist, Victoria Police Forensic Services Department, Australia
[b] Biological Services Group, Victoria Police Forensic Services Department, Australia

ARTICLE INFO

Article history:
Received 27 February 2018
Received in revised form 10 October 2018
Accepted 17 October 2018
Available online 26 October 2018

Keywords:
Blood Pattern Analysis
Impact bloodstain patterns
Forensic science
Crime scene

ABSTRACT

Bloodstain evidence can be very powerful evidence in assault related crimes. Determination of the distance that blood droplets may travel as a result of an impact into liquid blood may be of significance to corroborate or disprove a version of events, provide likely scenarios, or help determine the culpability of a person in determining their proximity to the blood shedding event. It was the aim of this research to determine the potential maximum distance blood droplets travel horizontally following a vertical impact into liquid blood. A custom apparatus was designed and constructed to replicate a vertical impact of a timber weapon, rotating on a fixed axis at one end, striking a pool of liquid blood. The device was positioned at three different levels of elevation to replicate an impact to the head of a person near ground level, a seated or kneeling height and standing height. Overall, the results indicated that the application of kinetic energy of between 1 and 5 J at a height of 1780 mm led to the blood droplets travelling a maximum horizontal distance of 5361 mm (and average maximum distance of 4981 mm). The horizontal distance blood droplets may travel upon impact does not appear to follow a linear trend with differing kinetic energy, but is affected by the applied force and release height in a curvilinear relationship. The results provide a valuable tool to bloodstain pattern analysts and investigators in determining search zones within a scene, as well as providing information about the proximity of an individual to an impact event.

1. Introduction

Bloodstains can be one of the most common forms of biological evidence located at assault related crime scenes. Bloodstains can assist us in indicating *who* was involved in an assault via DNA profiling, however bloodstain pattern analysis (BPA) may assist in determining *where* and *how* the blood shedding event occurred. With a high proportion of physical assaults that result in death coming from blunt force injuries [1], the physical characteristics of bloodstains can be powerful evidence. Bevel and Gardner [2] state that "*bloodstain pattern analysis is based on a very simple theory: blood as a fluid will react to external forces in a predictable fashion*". This theory sets the premise for BPA, in that the patterns are reproducible under similar physical conditions [3] and as such the physical characteristics of the bloodstain patterns can reflect the nature of events that produced them.

The analysis of the size, shape, location, and distribution of bloodstains can assist with information on how they were deposited [4] and BPA often plays a role in supporting or refuting statements of the victim, suspect or witness [3]. For example, determining the volume and impact velocity of small bloodstains may assist determining the position of where they originated [5], potentially providing information about whether the blood staining on a suspect's clothing could have been deposited as a result of rendering first aid [6] or being a bystander. In recent times the reliability of BPA methodology has been heavily scrutinised by the courts and the scientific community. The National Research Council report in 2009 [7] included the suggestion that an understanding of the physics of fluid transfer was required for bloodstain pattern interpretation and reconstruction and that the "*uncertainties associated with bloodstain pattern analysis are enormous*". The fundamentals of fluid dynamics relating to BPA have been explored and certain aspects identified as requiring further work to increase the understanding in this field have been identified [8,9]. Subsequently, there has been a significant increase in BPA research to explore the accuracy and reliability including a comparative review of fluid dynamics and BPA [8] that highlight the links between them.

Historically much of the research in BPA has focused on determining the area of origin, defined as "*the space in three dimensions to which the trajectories of spatter can be utilized to*

* Corresponding author at: Office of the Chief Forensic Scientist, Victoria Police Forensic Services Department, Macleod, Victoria 3085, Australia.
E-mail address: christopher.flight@police.vic.gov.au (C. Flight).

https://doi.org/10.1016/j.forsciint.2018.10.015
0379-0738/

determine the location of the spatter producing event" [10]. A numberof recent studies have focused on improving knowledge and accuracy for areas including (but not limited to) position determination [5], the dynamics of blood release and formation of cast-off patterns [11], numerical models for forward blood droplet trajectory predictions [12] and back spatter from gunshots [13].

A common legal argument exists as to whether the blood-staining located on a defendant [4] puts them in close proximity to the victim at the time of the assault. Several crime scene cases known to the authors of this study involved the defense that the blood spatter stains located on the suspect's clothing was the result of being some distance from the assault, not through direct involvement. This has led to the identification of a gap in practical empirical studies measuring the distance that blood droplets can travel as a result of a blunt impact (excluding gunshots).

All recorded results from published peer reviewed studies reporting the distances that impacted blood droplets have travelled appear to have been incidental or secondary to the aim of their research. MacDonnell and Bialousz [14] examined a variety of aspects of bloodstain properties and dynamics, being the first to document the distance that blood travelled from origin caused by medium to high velocity impact forces from a motor driven device. The maximum distance travelled was stated to be 3380 mm, but unfortunately little further empirical data was provided. Sweet [15] researched the velocity measurements of blood droplets from a medium velocity impact source, using a steel cylinder, in to a pool of liquid blood. Sweet noted bloodstains located on paper 820 mm above and 430 mm away from the impact site. Ristenbatt and Shaler [16] reported on the bloodstain pattern analysis in a homicide case study where a victim was beaten about the upper body. This article reported the maximum height the blood recorded was 2700 mm and the maximum distance travelled horizontally was 1900 mm, however as a case study the variables surrounding the deposition of the blood were unknown and inestimable. Slemko [17] in a project titled "*The Effects of Droplet Velocity and Fabric Composition*" reported that the maximum distance travelled by blood droplets propelled by a high speed fan was recorded to be 3500 mm which was the limit of the test. More recently Attinger et al. [18] show figures with several bloodstains of between 1500 mm and 2000 mm from blood source to target, Laan et al. [5] reported creating impact spatters at a distance of 1000 mm and Kabaliuk et al. [12] reported a flight range of about 1530 mm.

The current practical study aims to investigate the mean and maximum horizontal distances that blood droplets travel following a vertical impact into liquid blood, under controlled conditions. Utilising a custom designed impact device, the effect of kinetic energy was explored at three different heights to replicate an impact inflicted to a person positioned lying on the ground, sitting/kneeling or when standing. The casework relevancy of these results would assist in determining the maximum horizontal range that a blood droplet could travel from an impact spatter event, allowing an assessment of the likelihood of an individual's proximity to the event. The experimental design was intended to replicate a range of situations and variables commonly encountered in casework, based on practical constraints and the need to control particular factors. This study was designed to achieve experimental results useful to casework, rather than to test or generate to theoretical or numerical models.

2. Materials and methods

2.1. Device design

An apparatus was designed and built to create a range of controlled strikes to impact liquid blood pools using a length ($1000 \times 90 \times 45$ mm) of F17 hardwood timber (Fig. 1) rotating about an axle at one end. A timber frame was built around the base of a sheet of form ply board ($1200 \times 600 \times 20$ mm) using pine timber (90×45 mm). A metal bracket and several metal corner joiners supported a length of pine timber placed centrally and vertically at the end of one of the form ply boards. A quarter circle shaped piece of marine ply was placed on the opposite side of the metal bracket with two pieces of pine secured on the upper sides of the form ply to support the threaded metal rod which was inserted through the hardwood timber "weapon".

A length of F17 hardwood timber was used as the "weapon" arm. This timber was specifically selected to have an even flat edge, high strength and high density value. A piece of hard, flat marine plywood, with a varnished upper surface, was placed on the base of the form ply board where the distal end of the F17 timber striking arm was to impact. A hole was drilled horizontally through the proximal end of the F17 timber (Fig. 2) through which a threaded metal rod was inserted (at the rotating point) providing a perfectly level join when the F17 timber arm came together with the impact striking surface. Bearing flanges and bearing washers were utilised to allow for a smoother movement of the arm with less friction.

A metal spring (Century brand $\frac{5}{8}\times$ $6\frac{1}{2}$ in. extension) was connected to the F17 timber arm via a counter sunk metal eye hook (Fig. 2), and attached to another threaded metal rod running beneath the ply form board through a hole cut in the form ply board (Fig. 3). The placement of the spring ensured that at rest, the spring was in the neutral position (i.e. no tension applied).

The base and legs of the device were made from a second sheet of framed form ply, with the same dimensions as the top. Three lengths of pine timber (200 mm, 1000 mm and 1800 mm) were used as supports to the impacting device (on the upper form ply board) at three different impact surface heights (Fig. 4). Two 20 kg bags of sand were placed in the base of the apparatus to maintain stability and prevent movement of the device upon impact.

Incremental slots with shaft bearing flanges were positioned on the semi-circular bracket at various positions to control the starting angle of the F17 timber arm. The F17 timber arm was held in place by the stainless steel rod being inserted through the bearing flanges. The rod was removed by quickly pulling the attached rope releasing the arm and allowing it to travel in a downward arc to impact level with the plywood strike surface (Fig. 5).

2.2. Trial pilot study

A pilot study was conducted to determine the approximate distance the blood droplets could travel as well as their direction of

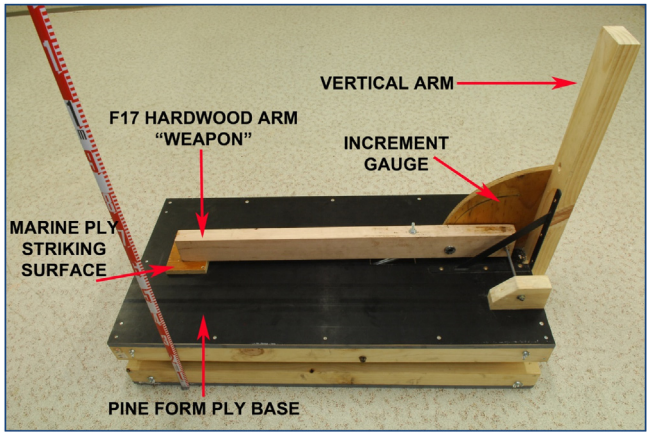

Fig. 1. Blood striking device.

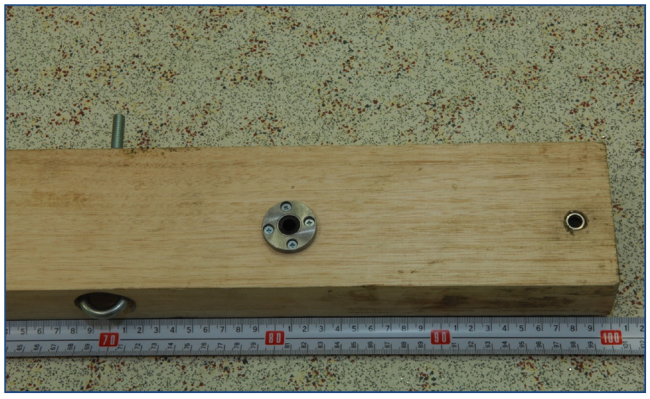

Fig. 2. Proximal end of arm with bearings and counter sunk metal eye hook.

spread, with a number of preliminary tests conducted using pig blood. The dimensions of the trial room were 6400 × 6400 × 3000 mm. No blood was observed on the ceiling during or after the testing. The spread of blood droplets from impact was determined to be in the approximate range between 300° and 360° in front of the device.

The placement of the incremental slots was based on the impact velocity and spread of the blood during the pilot study. The initial minimum position for the arm (C) was identified based on the smaller spread and distance travelled and the maximum position (G) by the smallest droplets. The remaining three increments (D, E and F) were placed at equidistant positions on the marine ply bracket between the minimum (C) and maximum (G) positions (Fig. 5).

During further testing, it was noted that the previously identified minimum position (C) was generating a relatively high velocity and kinetic force, which resulted in all five initially selected increments producing similar bloodstain sizes and distances. Therefore, two incremental slots (A and B) were added during the course of testing.

2.3. Impact force

Prior to attaching the arm to the device, it was weighed using a Mettler Toledo SB32001 DeltaRange electronic scale (including the bearings and countersunk metal eye hook) to obtain the total mass of 2.1925 kg (***m***).

As the F17 timber arm was rotating around a fixed axis, calculations were required to determine the angular momentum, the final velocity of the arm's centre of mass and the kinetic energy that would be transferred from the arm to the liquid blood. A Mecmesin BFG 50 N basic force gauge was used to record the force (F_1) applied to the arm by the spring at each of the seven increments (A–G). The displacement of the spring from the rest position (***x***) to increment positions A–G were also recorded. The height from the centre of mass (half way between the axis point and the distal end of the arm) was marked and the vertical distance between the start and the end position of the arm was recorded (***h***). Knowing the distance from axis to the spring anchor point on the arm (0.28 m) and the force applied to the arm by the spring at each increment, the downward force (F_p) applied to the arm by the spring at the centre of mass (0.49 m) could be calculated for each increment ($0.28F_1 = 0.49F_p$). Refer to Fig. 5 for visual identification of key locations.

Fig. 3. Spring attachment between the arm and the metal rod.

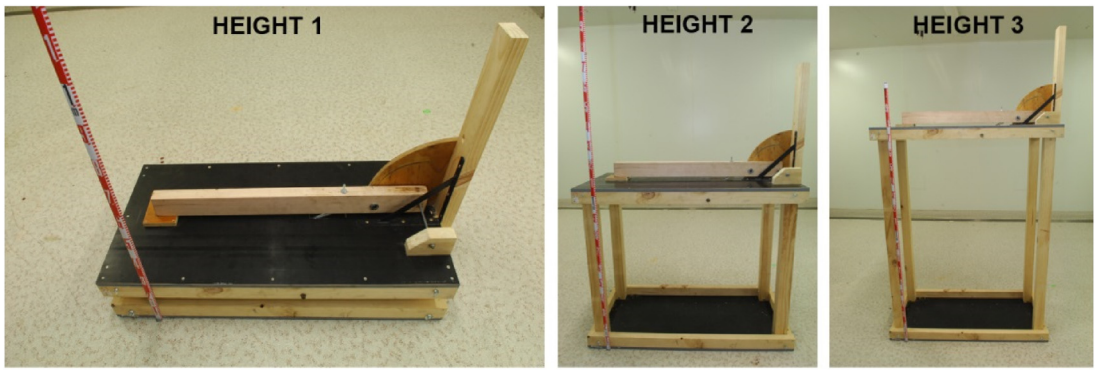

Fig. 4. Apparatus at Height 1 (Impact surface 250 mm from ground), Height 2 (Impact surface 1160 mm from ground) and Height 3 (Impact surface 1780 mm from ground) prior to the increments being fixed in place.

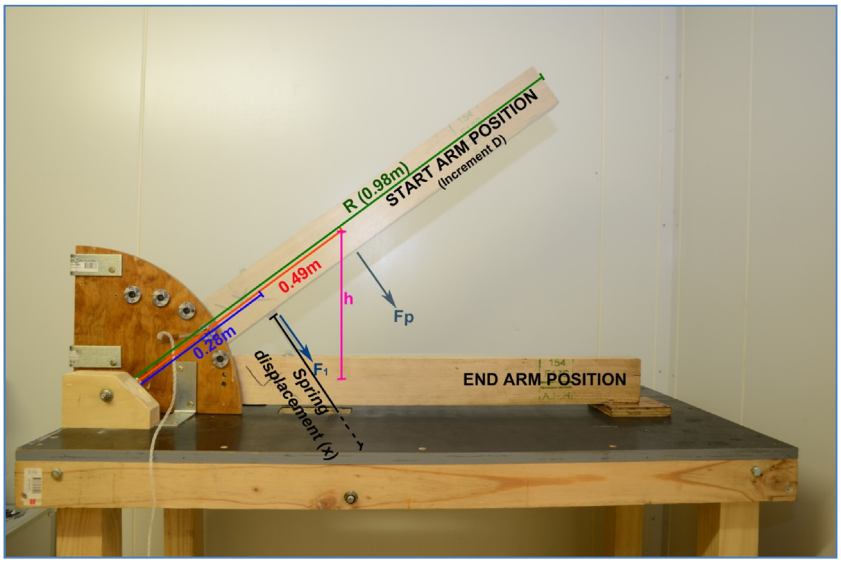

Fig. 5. Apparatus with key physics positions identified.

The potential energy in the arm at the increment positions prior to release consists of the potential energy of the arm in its centre of mass and the energy in the spring, given by the force applied by the spring to the centre of mass (F_p) and its displacement (x):

$$\textit{Energy}\ (\textit{starting position}) = mgh + F_p x$$

The rotational kinetic energy (*KE*) applied to the liquid blood was calculated by using the assumption that the moment of inertia of the arm was the same as that of a rod rotating about one end with the formula $1/3\ mR^2$.

$$\textit{Energy}\ (\textit{ending position}) = \frac{1}{6} m v^2$$

Applying the law of conservation of energy to calculate the final velocity v of the centre of the arm's mass:

$$v = \sqrt{\frac{6}{m}(mgh + F_p x)}$$

After the velocity was calculated the kinetic energy applied to the liquid blood could be determined.

Refer to Table 1 for the velocity and kinetic energy calculations.

2.4. Blood

Anticoagulants are necessary to prevent the onset of coagulation that better represents the physical properties of blood at the time of the assault [3] and as such have been used in many bloodstain pattern research studies. There are a number of different anticoagulants that have been used in BPA studies including ethylenediaminetetra-acetic acid (EDTA), which has been reported as being suitable to prevent coagulation [19].

The physical properties of porcine blood, including hematocrit range and shear viscosity of whole blood and plasma, closely resemble that of human blood [18–20]. Its use up to two weeks old has been shown to be similar to the behaviour of freshly spilt human blood providing it had been collected directly into EDTA anti-coagulant bottles and incubated at 4 °C for that period [21]. It is however recommended to use the porcine blood as soon as possible after its collection to limit the possibility of change within the blood properties [22].

Two litres of fresh pig blood was sourced directly into a 2 l plastic container with 3.0 g of EDTA. The blood was transported directly to the laboratory in a thermally insulated case and placed into a water bath maintained at ~37 °C [20]. The water bath was set to shake to keep the blood moving to prevent separation and settling of erythrocytes [22]. Care was taken not to deviate from ideal circumstances by controlling the temperature of the blood, reducing the time the blood was exposed to the air, indoor testing to reduce air currents and using a well-defined quantity of blood.

2.5. Experimental test area

A large enclosed storage shed with a level horizontal concrete floor was used for the experimental testing. The dimensions of the test room were 9845 mm wide, 9545 mm long with a minimum ceiling height of 4666 mm (pitched roof maximum height of 5340 mm). All exposed surfaces (walls and floor) of the experimental room were lined with plastic drop sheets for health and safety reasons and ease of cleaning. The floor was further lined with lengths of butcher paper from roles, which was replaced after each test. The apparatus was placed at one end of the room to allow

Table 1
Determination of velocity and kinetic energy.

Increment	F_1 (N)	Spring displacement x (m)	F_p (N)	Height h (m)	Velocity v (m/s)	KE (J)
A	4.84	0.005	2.77	0.005	0.58	0.12
B	6.55	0.018	3.74	0.057	1.88	1.29
C	11.33	0.060	6.47	0.146	3.11	3.53
D	21.28	0.149	12.16	0.290	4.69	8.05
E	32.48	0.237	18.56	0.403	5.98	13.06
F	41.80	0.319	23.89	0.465	6.94	17.63
G	50.29	0.390	28.74	0.477	7.66	21.46

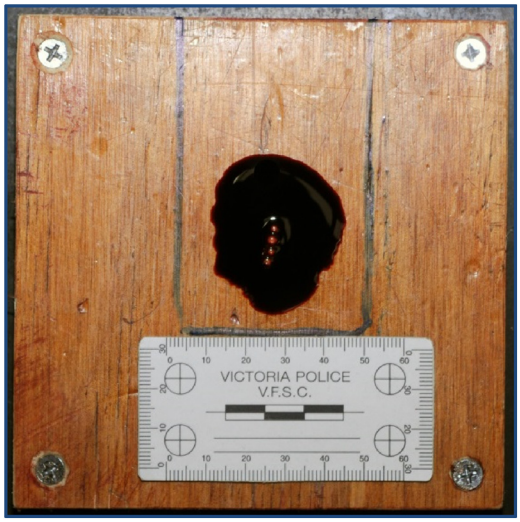

Fig. 6. ~1 ml liquid blood (within the strike zone marked with blue marker pen) on the marine ply strike surface.

for 7000 mm space in front of the device (in the approximate range of a 300–360° arc).

2.6. Experimental protocol

For each trial, ~1 ml of blood was taken from the pig blood container in the water bath container using a 10 ml syringe and deposited on the flat plywood impact surface within the strike zone (i.e. the area directly impacted by the F17 timber arm outlined by marker in Fig. 6). Within seconds of placement, to minimize heat loss from the blood, a controlled impact was applied to the blood pool by releasing the F17 timber from its starting position at each increment. Each impact on the device was video recorded by using a GoPro camera on a tripod with a timer on an Apple iPad Air displayed.

After each impact the furthest lying visible single bloodstain was located and measured horizontally to the point of origin (distal end of the F17 timber) using a Hilti PD42 laser measurer. To ensure accurate measurement, a vertical pole from the bloodstain was used to guide the position of the laser measurer. A high resolution image using a Nikon D300 dSLR camera was also taken from directly above the blood stains (Fig. 7). The F17 timber arm and strike plate were cleaned of blood residue after each test.

Five replicates were performed at increments A and B at Height 1 (250 mm from floor), and ten replicates for increments C–G. Due to results obtained at this initial height, increments F and G were not tested at greater heights. Therefore, five replicates were performed for A and B and ten replicates for increments C–E for both Heights 2 (1160 mm from the floor) and 3 (1780 mm from the floor), resulting in a total of 140 impacts across the three heights. Visual analysis of the ceiling of the room was also conducted to determine if any stains had reached that height. The distance data obtained was analysed in real-time during the experiment for consistency and variation, with one sample t-tests being used to test datasets within each increment to determine if additional replicates were required to generate reliable results. Each group of replicates was also checked during experimentation for normality, skewness and kurtosis, with z-tests being used to determine the equality of variances between adjacent groups (increments and heights) during testing.

Statistical analysis was performed in SPSS v21.0 (IBM Corporation, Chicago). The consistency of impact time and therefore kinetic energy across the repeated experiments was investigated using a repeated measure analysis of variance (ANOVA), comparing before and after time measurements. A two-way ANOVA was conducted to compare the main effects and interaction of the ordinal variables height and increment on the furthest distance blood travelled.

3. Results

3.1. Kinetic energy released during impact

The characteristics of the timber arm, spring and increments were measured to calculate the final velocity of the arm and the kinetic energy imparted to the blood stain upon impact (Table 1). The consistency of impact kinetic energy was investigated by measuring the time taken for the F17 timber arm to travel from release to impact prior to the experiments across 5–10 replicates per increment, and the corresponding time post-experiment with 10 replicates per increment (Table 2). A repeated measures ANOVA indicated that no significant differences existed between the pre- and post-experiment times overall ($F^2_{,53} = 0.066$, $p = 0.798$), and that there was no differential changes in travel times between increments ($F^6_{,53} = 1.35$, $p = 0.252$). It can therefore be inferred that the time taken for the F17 timber arm to travel, and therefore the kinetic energy imparted, was consistent throughout the experiment.

3.2. Experimental test results

The impact height and kinetic energy imparted both influenced the distance the blood travelled after impact. Impact heights of 250 mm resulted in distances ranging from 2109 mm to 3404 mm (Table 3), with an overall average of 2835 mm across all seven increments and 2109 mm from the lower five. Impact heights of 1160 mm resulted in distances travelled of 2895 mm–4850 mm, with an average of 3732 mm from the lower five increments. Impact heights of 1780 mm resulted in blood droplets travelling between 3256 mm and 5361 mm, with an average of 3901 mm.

Both the height and increment had significant effects on the distance that the blood travelled (height $F^2_{123} = 281.92$, $p < 0.01$; increment $F^6_{123} = 58.17$, $p < 0.01$), with height showing a greater effect ($\eta^2 = 0.43$) than the increment ($\eta^2 = 0.27$). There was also a small but significant interaction between the height and increment ($F^8_{123} = 6.24$, $p < 0.01$), although this interaction had a minimal effect size ($\eta^2 = 0.04$).

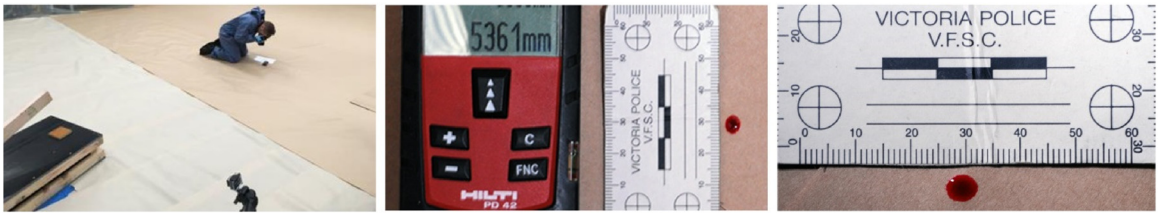

Fig. 7. Images of the recording process and results from Height 3 Increment B (furthest recorded bloodstain in experiment).

Table 2
Impact time pre-test and post-test.

Increment	Pre-test time average *t* (s)	Post-test time average (s)
A	0.062	0.055
B	0.124	0.122
C	0.163	0.172
D	0.234	0.249
E	0.305	0.303
F	0.36	0.361
G	0.431	0.428

Fig. 8 is a boxplot of the furthest distance travelled by increment. The boxes represent the 25th–75th percentiles (the interquartile range – IQR) and thick black line the median of each group. Whiskers indicate 1.5× the IQR, while dots represent outliers greater than 1.5× the IQR. There is clear separation between the three heights at the lowest increment, separation between Height 1 and Heights 2 and 3 at the second and third increments, overlapping between the distributions of distances at the higher increments, demonstrating the interaction between height and kinetic energy on the distances blood droplets may travel upon impact.

Post-hoc testing with Bonferroni correction indicated that the distance travelled by blood impacted at greater height differed significantly compared to lower heights, with mean distances increasing from 2837 mm at Height 1, to 3778 mm at Height 2, to 4117 mm at Height 3 (all pairwise p-values <0.05). In contrast, increasing increments, and therefore the kinetic energy imparted, did not show a consistent linear relationship. Post-hoc testing demonstrated that Increments B and C had greater distances ($p < 0.05$) than Increments A, D, E, F and G, with the latter increments forming a homogenous group with regards to distance (all $p > 0.05$). Spline interpolation (Fig. 9) and regression modelling (data not shown) indicated that the distance travelled by blood droplets under different kinetic energies follows a cubic trend, with low distances at low energies, increasing rapidly when the kinetic energy is ~1–5 J, and decreasing to previous levels above this energy level. Further research, particularly at lower energies, may clarify the nature of this curvilinear relationship.

4. Discussion

This research was designed to determine the maximum horizontal distance blood droplets will travel through the air from a vertical impact into liquid blood. Whilst not possible to replicate and control many of the variables associated with an impact, it is important in any research of this nature to know that the blood being used approximates human blood leaving the body. To assist in achieving this, fresh pig blood was used with EDTA anticoagulant, the blood was kept at a temperature of ~37 °C prior to placement on the impact device. Testing commenced within 24 h of the collection of the blood and was completed within 72 h.

Table 3
Maximum blood spatter horizontal distance measurements (mm) per increment and height. The maximum distance achieved for each increment is italicized and bold, minimum is underlined.

Height	Replicate	Increment						
		A	B	C	D	E	F	G
Height 1	1	2109	3057	3129	2591	3160	2970	2695
	2	***2768***	***3404***[a]	2852	2573	***3195***	2766	2586
	3	2273	3400	3295	3144	2955	2753	2689
	4	2507	3375	3241	2751	2693	2443	***2874***
	5	2314	3313	3243	2630	2624	2887	2545
	6	–	–	3139	2890	2639	2452	2627
	7	–	–	***3296***	2627	2652	***3134***	2673
	8	–	–	3019	2976	2673	2562	2745
	9	–	–	3268	2702	2614	2648	2544
	10	–	–	3164	***3257***	2564	2700	2735
	Average	2394	3310	3165	2814	2777	2731	2671
	Standard deviation	252	146	140	243	236	222	102
Height 2	1	3103	***4850***[b]	4477	***3775***	3177		
	2	3479	4599	4255	3611	3206		
	3	***3517***	4255	3992	3094	3604		
	4	3267	4680	3894	3018	2895		
	5	3280	4526	4182	3366	3459		
	6	–	–	4140	3254	***3695***		
	7	–	–	***4540***	3260	3226		
	8	–	–	4200	3764	3511		
	9	–	–	4234	3514	3256		
	10	–	–	3972	3690	3585		
	Standard deviation	170	219	208	276	249		
Height 3	1	4154	4972	4128	3722	3597		
	2	***4368***	4685	4466	4062	3693		
	3	3653	5155	4633	3781	3462		
	4	4017	4731	3789	***4149***	3800		
	5	3742	***5361***[c]	***4639***	3406	3453		
	6	–	–	4248	3779	3256		
	7	–	–	4337	3659	3705		
	8	–	–	4317	3286	3422		
	9	–	–	4225	3669	3465		
	10	–	–	4219	3957	***3893***		
	Average	3987	4981	4300	3747	3575		
	Standard deviation	294	285	250	269	197		

Note — dimensions of bloodstains (*length* × *width*).
[a] 7.2 mm × 2.1 mm.
[b] 8.2 mm × 5.2 mm.
[c] 5.8 mm × 4.9 mm.

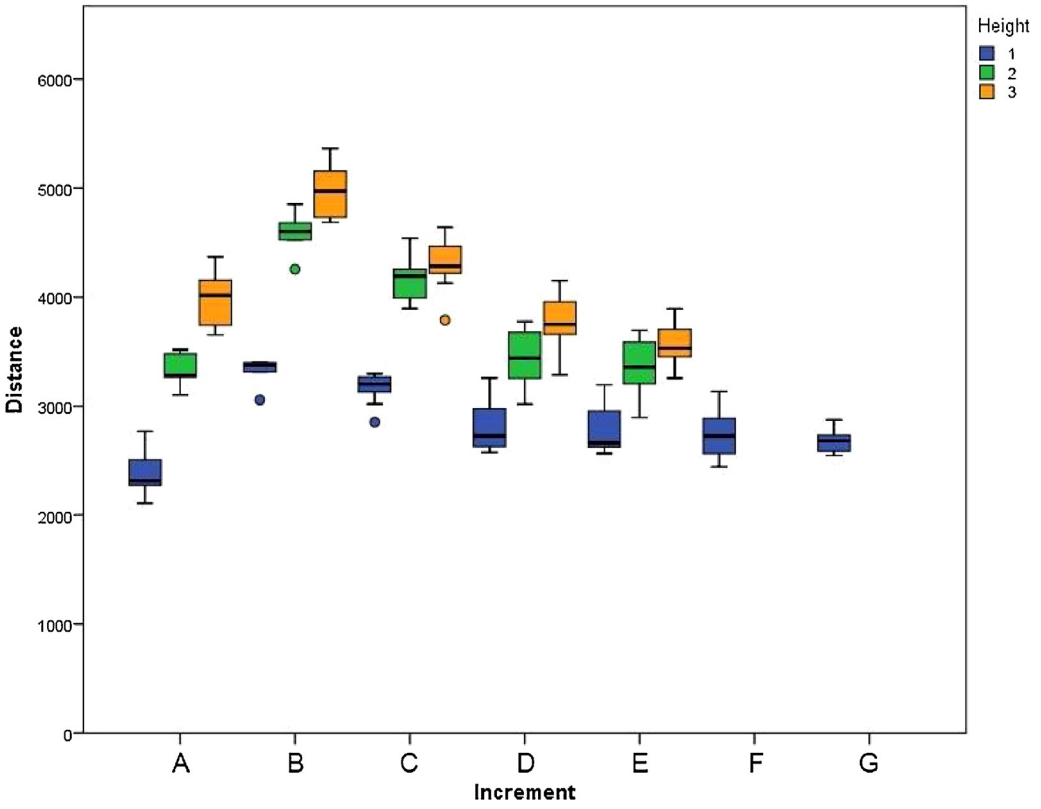

Fig. 8. Boxplot of the furthest distance travelled by increment.

The hematocrit and viscosity of the blood would have provided greater information regarding the rheology of the blood [18,24], although was unfortunately not available at the time.

A custom built mechanical apparatus was used where liquid blood was placed on a hard, flat timber surface and second hard, flat F17 timber arm impacted the entire volume of the blood pool. The two hard flat surfaces delivered a significant proportion of the total kinetic energy to the blood to achieve the best case scenario. The downward motion of the apparatus was controlled by a spring and was locked in place at several different increments to control the velocity of the impact and ultimately the kinetic energy. The device was set at three different heights — near ground level to

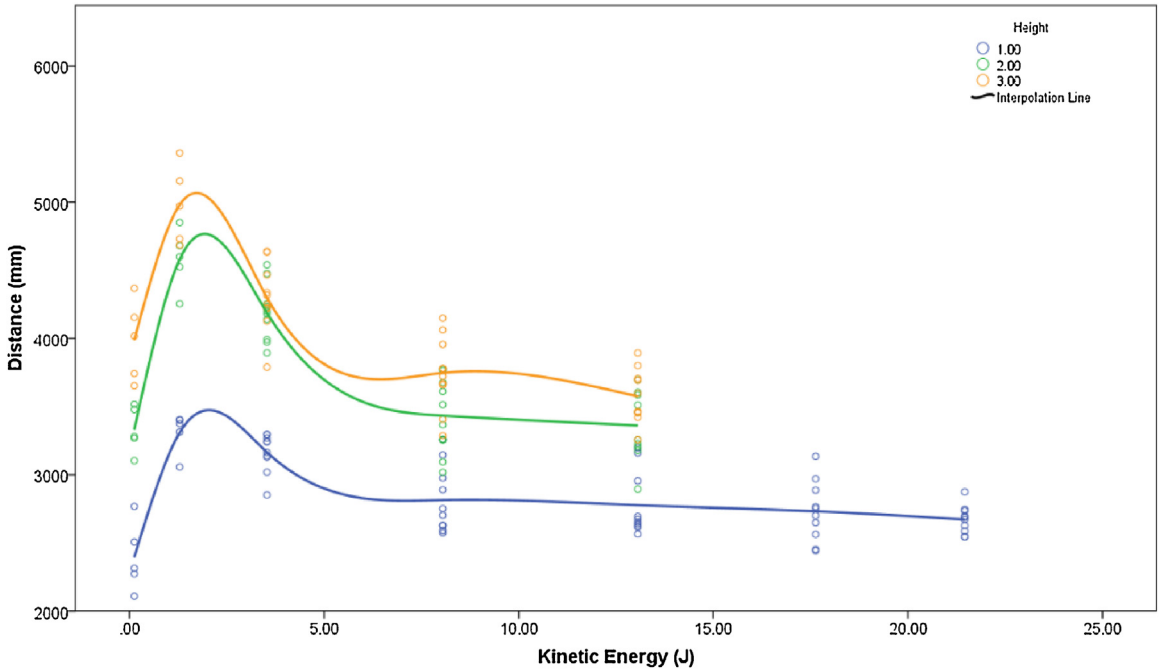

Fig. 9. Scatter plot of maximum distance travelled (mm) by the Kinetic Energy (joules) imparted at impact, with spline interpolation lines demonstrating the polynomial relationship between kinetic energy and distance.

replicate an assault of a person low to the ground (Height 1), approximate sitting, crouching or kneeling height (Height 2) and standing height (Height 3), as the height can be important indicator to a forensic investigator as it may indicate an offensive or defensive position [23,25].

The two hard flat surfaces coming together provided a very narrow space for the blood to escape (see Fig. 10) and it appeared that the majority of the blood travelled forward or to the side of the F17 timber arm in almost a 300–360° arc. Little blood appeared to travel back towards the rear of the apparatus, potentially being blocked by the arm only leaving the front and sides to escape. Within this research, the angular distribution of stains was not recorded, as the focus was on distance rather than direction. However, it was noted that the majority of most distant stains were estimated to be between 300-360° in front of the impact plate. Several instances were however noted at more extreme angles, indicating that further research regarding the distribution of blood droplets may be instructive.

Prior to this research project being undertaken, the furthest recorded distance, identified by the authors, in a published journal was 3380 mm by MacDonnell and Bialousz [14]. It can be established from the results of this research project that these distances can be expanded to 5360 mm and is more consistent with the prediction of James [26] that blood may potentially travel up to approximately 6000 mm, although it is unknown how this figure was determined.

4.1. Kinetic energy

This research discovered that the change in kinetic energy followed a cubic trend with low distances travelled at low energies, increasing rapidly when the kinetic energy was increased to between 1 and 5 J and decreasing again when above this energy level (i.e. above 5 J). When a disruptive external force is applied to liquid blood, liquid sheets and ligaments are forced out [5] and when the cohesive surface tension forces of the liquid blood/air interface are exceeded droplets will separate [11]. Dependent on the level of force applied to the liquid blood, the droplets may further deform in flight into a "*bag- or dumbbell-like shape*" before breaking up into smaller droplets which may have significant effects on the overall drag force [12]. Once separated the blood droplets follow a trajectory dictated by the velocity and by the combined forces of gravity and drag [11,12]. Due to drag, the velocity of the blood droplet decreases as it flies through the air [5] as the forces of gravity act upon it. A paper by Kabaliuk et al. [12] comprehensively details the fluid dynamics of blood droplets following an impact.

The low kinetic energy impacts in this experiment (<1 J) may have created less disruption of the liquid blood and therefore produced a larger blood droplet sphere with lower initial velocity and therefore more influenced by gravity, and to a lesser extent air resistance. The higher kinetic energy impacts applied to the blood in this experiment (>5 J) may have led to a larger initial velocity of blood droplets reducing the initial influence of gravity [25] but potentially slowing due to deformation into secondary droplets and subsequent effects from drag leading to a smaller flight range [12]. The medium kinetic energy (between 1 and 5 J) appeared to have created a higher velocity than the low kinetic energy impact but potentially resulted in less deformation allowing the droplets to travel further whilst subjected to the forces of gravity and drag.

4.2. Height

The height of the impacts appeared to have a more significant effect on the distance blood droplets travelled than kinetic energy alone. The blood from Height 3 travelled further than Height 2, which in turn was further than Height 1. Whilst Height 3 obtained the greatest distance, the significance of height cannot be underestimated in the context of an assault:

- At Height 1, replicating an assault on a person lying at approximately ground level, the maximum distance that the blood droplets travelled was at Increment B measuring 3404 mm from the point of impact (bloodstain dimensions 7.2 mm × 2.1 mm) with an average of 3310 mm.
- At Height 2, replicating a seated, crouching or kneeling person, the maximum distance achieved was 4850 mm (bloodstain dimensions 8.2 mm × 5.2 mm) with an average of 4582 mm achieved at Increment B.
- At Height 3, replicating a person of average height standing, the maximum distance being 5361 mm (bloodstain dimensions 5.8 mm × 4.9 mm) and an average of 4980 mm, again achieved at Increment B, these results were as previously identified the furthest of the three heights.

Based on the findings and observations of the experimental trials, it can be assumed that blood spatter droplets caused through an impact having lower trajectories (~250 mm heights) will travel shorter distances before impacting with the ground. The impacts at Height 2, replicating a kneeling or crouching height of a person, and Height 3, replicating a standing person, can be expected to create more distant blood stains due to the droplets being in flight for longer periods of time before making contact with the ground. These results support the findings of de Bruin et al. [25] with the higher elevation of the blood source, the blood droplets would have an increased flight time before they make contact with the ground.

4.3. Practical implications

When examining a scene of an assault the crime scene examiner and/or the bloodstain pattern analyst must determine the size of the scene. The general method is to start with the outermost stains and work inward, however this relies upon

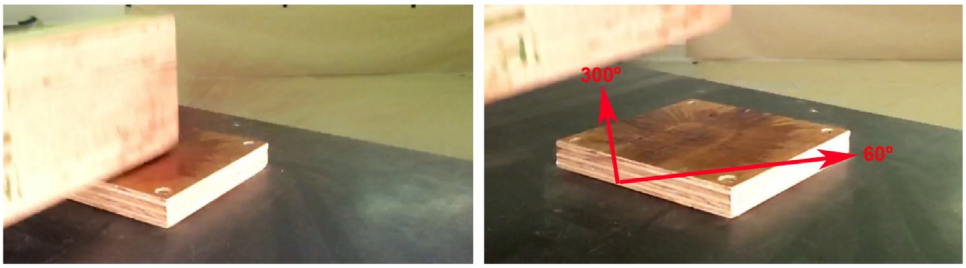

Fig. 10. View of the liquid blood on the strike plate during impact from the F17 timber arm (left), and post-impact stain (right). Arrows indicated the approximate 300–360° arc of the bloodstain travel.

knowledge of the potential greatest distance that blood droplets may travel in a variety of impact scenarios. Thus, with the knowledge that blood droplets can travel up to 5361 mm in an indoor environment, this range could assist scene examiners with the size of a search zone. It is acknowledged that further studies relating to the distribution of the bloodstains resultant from an impact into liquid blood at the various heights and applications of kinetic energy would add further value to the blood stain analyst.

Other forensic contexts of the results obtained may also include (i) establishment of a range that allows an assessment of the level of support that the blood stain evidence provides to different versions of events, for example if a witness states that the assault took place in a certain location but the bloodstain evidence was found outside the possible maximum deposition zone, or (ii) using the information may help determine proximity to the assault, and therefore potential involvement, of a suspect who states that they were some distance away, for example 15 m, yet spatter bloodstains were located on their clothing.

4.4. Research limitations

This research was designed to replicate blood distribution caused by impact, such as that occurring during an assault upon a person. Such events are highly dynamic, and it is not possible to fully replicate all variables that may occur in all possible situations. Experimental trials were conducted in controlled conditions to ensure consistency and allow comparison between the key variables of interest, namely impact height and kinetic energy. As such, the influence of variables such as differing amounts of blood, direction of force, the nature of the impact surface (curved/pliable), the impact of air currents or temperature, and the movement of impacted surface are unknown. As detailed earlier the hematocrit and viscosity of the blood were not recorded in this experiment and therefore potentially limited the experimental results. The tools used to record the research project results were also limited due to cost and availability. Such limitations included the use of an iPhone 6s the Slo-Mo (slow motion) function on its Camera application. Whilst it recorded at 240 frames per second a camera with much higher frame rates would have provided more accurate information.

5. Conclusion

The aim of this study was to identify the maximum horizontal distance a blood droplet would travel as a result of a vertical impact into liquid blood. Whilst there were several assumptions and limitations identified, the maximum average distance was recorded as 4981 mm with the maximum individual recording being 5361 mm. These distances provide a range to which blood droplets could be expected to travel horizontally as a result of an impact into liquid blood with a blunt weapon.

This research demonstrated that the application of kinetic energy between 1 and 5 J resulted in the formation of blood spatter stains at the furthermost distances from an impact into liquid blood. Kinetic energy levels either side of this range reduced the distance the blood travelled. An increase in height of the impact point had a significant effect on the distance the blood travelled with the height corresponding to a standing person recording the furthest distance. Combining kinetic energy of between 1 and 5 J with Height 3 resulted in the furthest deposit of blood.

The methodology presented in this study offers useful information to bloodstain pattern analysts, crime scene examiners and investigators when considering the bloodstain evidence in context of the scene and may help establish determining the circumstances of the assault event. These results may provide assistance with establishing a nexus between the crime scene and any offenders involved in the perpetration of the offence, the level of involvement of individuals, likely scenarios as to events, or evaluating the support the evidence provides to accounts given by witnesses and/or suspects.

Author contributions

CF, KB and MJ conceived and designed the experiment, CF & KB conducted the testing, collected and analysed the data and CF, KB & MJ wrote the manuscript.

Acknowledgements

The authors would like to thank Scott Harris and Ken Hutton for their assistance during the practical experiments, Dr Jan de Kinder for assistance with force calculations and to Dr Isaac Arthur at the Canberra Institute of Technology for assistance during the Graduate Certificate in Crime Scene Investigation program.

References

[1] C.G. Mole, M. Heyns, T. Cloete, How hard is hard enough? An investigation of the force associated with lateral blunt force trauma to the porcine cranium, Leg. Med. 17 (2015) 1–8.
[2] T. Bevel, R. Gardner, Bloodstain Pattern Analysis With an Introduction to Crime Scene Reconstruction, Third edition, CRC Press, Boca Raton, 2008.
[3] N. Basu, S.K. Bandyopadhyay, Bloodstain pattern analysis — a less explored domain, Int. J. Appl. Res. 3 (1) (2017) 200–211.
[4] M. Taylor, T.L. Laber, P.E. Kish, G. Owens, N.K.P. Osborne, The reliability of pattern classification in bloodstain pattern analysis, part 2: bloodstain patterns on fabric surfaces, J. Forensic Sci. 61 (November (6)) (2016).
[5] N. Laan, K. de Bruin, D. Slenter, J. Wilhelm, M. Jermy, D. Bonn, Bloodstain pattern analysis: implementation of a fluid dynamic model for position determination of victims, Sci. Rep. 5 (2015) 11461.
[6] M. Taylor, T.L. Laber, P.E. Kish, G. Owens, N.K.P. Osborne, The reliability of pattern classification in bloodstain pattern analysis, part 1: bloodstain patterns on rigid non-absorbent surfaces, J. Forensic Sci. 4 (July (16)) (2016).
[7] National Research Council, Strengthening Forensic Science in the United States: A Path Forward, The National Academy of Sciences, Washington, DC, 2009.
[8] D. Attinger, C. Moore, A. Donaldson, A. Jafari, H.A. Stone, Fluid dynamics topics in bloodstain pattern analysis: comparative review and research opportunities, Forensic Sci. Int. 231 (2013) 375–396.
[9] P.M. Comiskey, A.L. Yarin, D. Attinger, Hydrodynamics of back spatter by blunt bullet gunshot with a link to bloodstain pattern analysis, Phys. Rev. Fluids 2 (2017) 073906.
[10] OSAC BPA Subcommittee, Terms and Definitions in Bloodstain Pattern Analysis. ASB Technical Report 033, AAFS Standards Board, Washington, DC, 2017.
[11] E.M.P. Williams, E.S. Graham, M.C. Jermy, D.C. Kieser, M.C. Taylor, The dynamics of blood drop release from swinging objects in the creation of cast-off bloodstain patterns, J. Forensic Sci. (2018), doi:http://dx.doi.org/10.1111/1556-4029.13855 (in press).
[12] N. Kabaliuk, M.C. Jermy, E. Williams, T.L. Laber, M.C. Taylor, Experimental validation of a numerical model for predicting the trajectory of blood drops in typical crime scene conditions, including droplet deformation and breakup, with a study of the effect of indoor air currents and wind on typical spatter drop trajectories, Forensic Sci. Int. 245 (2014) 107–120.
[13] P.M. Comiskey, A.L. Yarin, S. Kim, D. Attinger, Prediction of blood back spatter from a gunshot in bloodstain pattern analysis, Phys. Rev. Fluids 1 (2016) 043201.
[14] H.L. MacDonnell, L.F. Bialousz, Flight Characteristics and Stain Patterns of Human Blood, Nile & CJ, New York, 1971.
[15] M.J. Sweet, Velocity measurements of projected bloodstains from medium impact velocity impact force, J. Can. Soc. Forensic Sci. 26 (1993) 103–110.
[16] R.R. Ristenbatt, R.C. Shaler, A bloodstain pattern interpretation in a homicide case involving an apparent stomping, J. Forensic Sci. 40 (1995) 139–145.
[17] J.A. Slemko, Bloodstains on Fabric — The Effects of Droplet Velocity and Fabric Composition, IABPA Newsletter, 2003, pp. 3–11 December.
[18] D. Attinger, Y. Liu, T. Bybee, K. De Brabanter, A data set of bloodstain patterns for teaching and research in bloodstain pattern analysis: impact beating spatters, Data Brief 18 (2018) 648–654.
[19] S. Petricevic, D. Elliot, Bloodstain pattern reconstruction — a hammer attack, Can. Soc. Forensic Sci. 38 (1) (2005) 9–19.
[20] J. Siu, F. Pender, F. Springer, W. Ristenpart, Quantitative differentiation of bloodstain patterns resulting from gunshot and blunt force impacts, J. Forensic Sci. 62 (September (5)) (2017).

[21] M.A. Raymond, E.R. Smith, J. Liesegang, The physical properties of blood — forensic considerations, Sci. Justice 36 (1996) 153–160.
[22] T.C. De Castro, M.C. Taylor, D.J. Carr, J. Athens, J.A. Kieser, Storage life of whole porcine blood used for bloodstain pattern analysis, Can. Soc. Forensic Sci. J. 49 (2016) 1–12.
[23] N. Hakim, E. Liscio, Calculating point of origin of blood spatter using laser scanning technology, J. Forensic Sci. (2016), doi:http://dx.doi.org/10.1111/1556-4029.12639.
[24] S. Kim, Y. Ma, P. Agrawal, D. Attinger, How important is it to consider target properties and hematocrit in bloodstain pattern analysis? Forensic Sci. Int. 266 (2016) 178–184.
[25] R.D. de Bruin, Improving the point of origin determination in bloodstain pattern analysis, J. Forensic Sci. 60 (2) (2011) 409–417.
[26] S.H. James (Ed.), Scientific and Legal Applications of Bloodstain Pattern Interpretation, CRC Press, Boca Raton, 1999.